Precast/Prestressed Concrete Sandwich Panels for Thermally Efficient Floor/Roof Applications

E. Henin, Ph.D., P.E., S.E., A.M.ASCE[1]; G. Morcous, Ph.D., P.E., A.M.ASCE[2]; and M. K. Tadros, Ph.D., P.E., M.ASCE[3]

Abstract: Precast concrete floor systems represent a major component of the cost and weight of precast concrete buildings. Hollow-core (HC) planking is considered the most common precast concrete floor system for residential and commercial buildings because of their economy, light weight, structural capacity, and ease of production and erection. However, the high thermal conductivity of HC planks hinders their use in radiant heated floor and roof applications where thermal insulation is needed. This paper presents the development of a precast/prestressed concrete sandwich floor panel that consists of an internal wythe of insulation and two external wythes of concrete similar to those used in sandwich wall panels. The main difference between the sandwich floor and wall panels is the design of shear connectors between concrete wythes to achieve full composite action under ultimate loads while simultaneously having an adequate creep resistance under sustained loads and acceptable deflection under live loads. Truss-shaped glass fiber-reinforced polymer ties, known as NU ties, were used as shear connectors because of their structural and thermal efficiency. The proposed floor panels have comparable weight and capacity to HC planks while being more thermally efficient and can easily be fabricated in standard casting beds with typical equipment, thus eliminating the high initial investment required for HC production. This paper presents the design, detailing, production, and testing of three 7.9-m-long (26-ft-long), 1.22-m-wide (4-ft-wide), and 200-mm-thick (8-in.-thick) specimens with 50-mm-thick (2-in.-thick) composite topping. The three specimens represent two different panel designs. One specimen has solid concrete ends and was designed for a total superimposed service load of 9.6 kPa (200 psf), whereas two specimens are fully insulated and designed for a total superimposed service load of 4.8 kPa (100 psf). The performance of the three specimens under flexure and shear loadings indicated that the proposed sandwich floor panels can achieve full composite action and have satisfactory structural performance and acceptable deflection characteristics. **DOI: 10.1061/(ASCE)SC.1943-5576.0000213.**

Author keywords: Floor system; Thermal efficiency; Sandwich panel; Shear connectors; Composite action; Prestressed concrete; Hollow core.

Introduction

Precast concrete floor systems have been developed to achieve quality, economy, and rapid construction requirements in residential and commercial buildings. Hollow-core (HC) planks are the most common precast concrete system for floors where flat soffit, long span, and light weight are needed (Federation International Du Beton Steering Committee 2000). HC planks are produced using specialized extrusion slip-form equipment to ensure consistency, high quality, and speed of production. The keyways between HC planks are grouted, and a composite cast-in-place (CIP) topping is placed to connect the planks and enhance their structural performance. Despite these advantages, HC planks have poor thermal insulation characteristics and require high initial investment for production equipment that is not readily available to all precast producers. Ribbed-slab precast panels have been recently used in residential building applications (Hanlon et al. 2009) as an alternative to HC planks. Ribbed-slab panels are shallow double-tee elements with a 50-mm-thick (2-in.-thick) concrete slab and 200-mm-deep (8-in.-deep) ribs, for a total depth of 250 mm (10 in.). These ribbed slabs can be easily produced using modified double-tee forms. Testing the ultimate flexural capacity of the ribbed-slab panels with dapped ends has confirmed the feasibility of use in floor systems. The ribbed-slab panels are economical, structurally efficient, and easy to produce. However, they do not provide either a flat soffit or thermal insulation. The current alternative is filigree wideslab precast panels, because they are thin RC slabs that have the required stiffness during erection (Mid-State Filigree Systems 1992) and steel lattice trusses that ensure composite behavior between the CIP concrete topping and the precast panel. The typical thickness of the 2.4-m-wide (8-ft-wide) prefabricated filigree wideslab is 57 mm (2.25 in.), but the total thickness of the precast panel and CIP topping varies because of the spans. The panels are structurally efficient and easy to produce with a flat soffit that eliminates the need for a false ceiling. The main disadvantages of this system are the low thermal insulation, low handling stiffness, and need for CIP composite topping in all applications.

Conversely, precast concrete sandwich panels (PCSPs) have been used for several decades in wall construction because of their

[1]Structural Engineer, Ebmeier Engineering, LLC, 58187 250th St., Glenwood, IA 51534; and Assistant Professor, Assiut Univ., Assuit, Egypt 71515.

[2]Associate Professor, Durham School of Architectural Engineering and Construction, Univ. of Nebraska–Lincoln, Omaha, NE 68182 (corresponding author). E-mail: gmorcous2@unl.edu

[3]Principal, e-construct, LLC, 11823 Arbor St., Omaha, NE 68144; and Emeritus Professor of Civil Engineering, Univ. of Nebraska–Lincoln, Omaha, NE 68182.

Note. This manuscript was submitted on April 29, 2013; approved on November 1, 2013; published online on November 6, 2013. Discussion period open until July 26, 2014; separate discussions must be submitted for individual papers. This paper is part of the ***Practice Periodical on Structural Design and Construction***, © ASCE, ISSN 1084-0680/04014013(13)/$25.00.

structural and thermal efficiency. A typical PCSP consists of an internal wythe of insulation [e.g., extruded polystyrene (XPS)] and two external wythes of concrete that are connected through the insulation using shear connectors. PCSPs can be designed as either noncomposite, partially composite, or fully composite panels depending on the type and distribution of the shear connectors. These connectors can be concrete webs or blocks, steel ties, plastic ties, or any combination of these components (Al-Einea, et al. 1991). The low thermal resistance of steel and concrete connectors makes them unattractive whenever energy efficiency is crucial. A new shear connector, known as the NU tie, was developed and patented by researchers at the University of Nebraska–Lincoln (UNL) on August 15, 1995 [M. K. Tadros, D. C. Salmon, A. Einea, and T. D. Culp, "Precast concrete sandwich panels," U.S. Patent No. 5,440,845 (1995)]. NU ties are truss-shaped glass fiber–reinforced polymer (GFRP) ties with excellent thermal and mechanical properties that provide fully insulated and fully composite PCSPs. For details on the use of NU ties in wall panels, refer to Song et al. (2009), Morcous et al. (2010, 2011), and Hanna et al. (2011).

This paper presents the development of PCSPs for radiant heated floor and roof applications. The proposed PCSP panels were developed to address the shortcomings of the existing precast floor systems by being thermal insulated, lightweight, structurally efficient, and easy to produce with no specialized equipment. The main difference between the design of PCSPs in walls and floors is the type and direction of loading. Wall panels are primarily subjected to axial dead and live loads and perpendicular wind load. Floor panels are primarily subjected to perpendicular dead and live loads and no axial load. The loads on the developed PCSP floor panel could result in high stresses in the GFRP shear connectors because of sustained loads and higher deflections caused by live loads. Sustained stresses could represent challenges in designing GFRP ties as they tend to creep under low stress levels. Also, the low stiffness of GFRP ties could result in excessive deflections that may exceed the deflection limits for building floors.

The paper is organized as follows. The first section presents the structural analysis and detailing of two floor panel designs (Design A and Design B). The thermal efficiency calculations for the two panel designs are presented in the second section. The third section presents the production of three full-scale specimens: Specimen A1, which follows Design A; and Specimens B1 and B2, which follow Design B. The fourth section discusses the experimental investigation conducted on the three specimens and compares their performance. The last section summarizes research conclusions and recommendations. The experimental investigation presented herein is limited to flexural and shear testing of the proposed floor system. Testing for fire resistance, fatigue behavior, and seismic loads has not been conducted.

Structural Analysis and Design of the Proposed PCSP for Floors

Panel Designs A and B were analyzed and detailed for the following two loading conditions: Panel Design A was proportioned for a total service load of 9.6 kPa (200 psf) (e.g., storage rooms and stages), and Panel Design B was proportioned for a total service load of 4.8 kPa (100 psf) (e.g., computer rooms and corridors). Both panel designs are for 7.9-m-long (26-ft-long), 1.22-m-wide (4-ft-wide), and 200-mm-thick (8-in.-thick) precast planks longitudinally pretensioned using Grade 1860 (270) low-relaxation prestressing strands. A 50-mm-thick (2-in.-thick) composite CIP concrete topping was added after panel erection. In Panel Design A, seven 15-mm-diameter (0.6-in.-diameter) strands were used because of the unavailability of 13-mm-diameter (0.5-in.-diameter) strands at the time of panel fabrication; however, the strands were tensioned to the same level as a 13-mm-diameter (0.5-in.-diameter) strand [137.9 kN (31 kips) per strand]. In Panel Design B, four 13-mm-diameter (0.5-in.-diameter) strands were used and tensioned to 75% of the ultimate strength [137.9 kN (31 kips) per strand].

Figs. 1 and 2 show the plan, cross section, and sectional elevation of the two panel designs along with their reinforcing details and NU tie arrangements. Panel Design A required 0.305-m-long (1-ft-long) solid concrete end blocks and 36 No. 10 (#3) NU ties with nonuniform distribution to resist horizontal shear and control the panel deflection (Henin et al. 2011). Panel Design B required 24 No. 10 (#3) NU ties uniformly distributed along the panel and no solid concrete end blocks, which simplify panel fabrication. Another difference between the two designs is that Panel Design A has 200-mm-deep (8-in.-deep) NU ties that project 2.5 mm (1 in.) into the cast-in-place concrete topping to enhance the composite action, whereas Panel Design B has 178-mm-deep (7-in.-deep) NU ties that are embedded 50 mm (2 in.) into the top and bottom concrete wythes, which simplifies finishing the top wythe. There are no ties connecting the CIP composite topping and the PCSP in Panel Design B. The number of NU ties was determined based on two criteria: (1) ultimate stress in each NU tie leg under factored load ($1.2D + 1.6L$) does not exceed the ultimate strength [758.4 MPa (110 ksi)] multiplied by resistance reduction factor (0.75), interaction factor (0.65), and exposure factor (0.7); (2) ultimate stress in each NU tie leg under factored sustained load ($1.4D$) does not exceed the creep strength, which is 20% of the ultimate strength [151.7 MPa ($110 \times 0.20 = 22$ ksi)] multiplied by resistance reduction factor (0.75). For detailed calculations of panel design, please refer to Henin (2012).

To predict the dead and live load deflections of the two panel designs under different loading conditions, two modeling methods were investigated. In the first method, the panel is modeled as a planar truss in which the top-chord members represent the top wythe, bottom-chord members represent the bottom wythe, and diagonal members represent NU tie legs. Fig. 3 shows the planar truss models developed for Panel Designs A and B. In the second method, the panel is modeled using a three-dimensional (3D) finite-element (FE) model in which the top wythe and topping and bottom wythe are modeled as shell elements, and NU tie legs are modeled as frame elements. Fig. 4 shows the FE models developed for the Panel Designs A and B. In both modeling methods, elements are assumed to be located at the centerlines of actual elements and have the equivalent section properties. Connections between diagonal members and the chord members are assumed to be pinned with rigid end zone equal to the portion of tie leg that is embedded in the solid concrete block. For each panel design, the self-weight, prestressing, and topping weight were applied to the precast panel only, whereas the service loads [9.6 kPa (200 psf) for Panel Design A and 4.8 kPa (100 psf) for Panel Design B] were applied to the precast panel with 50-mm-thick (2-in.-thick) composite topping.

The deflections predicted using the planar truss models and 3D FE models are very comparable and hence not separately listed in Table 1. These deflection are also compared against those predicted using the conventional beam method assuming a fully composite section at different loading conditions as shown in Table 1. This latter comparison indicates that there is a significant difference between the deflections calculated using the conventional beam model and those predicted using truss/FE models especially in Panel Design B where the solid concrete end blocks were eliminated and fewer NU ties were used. This analysis is consistent with results previously obtained for sandwich wall panels (Morcous et al. 2010, 2011).

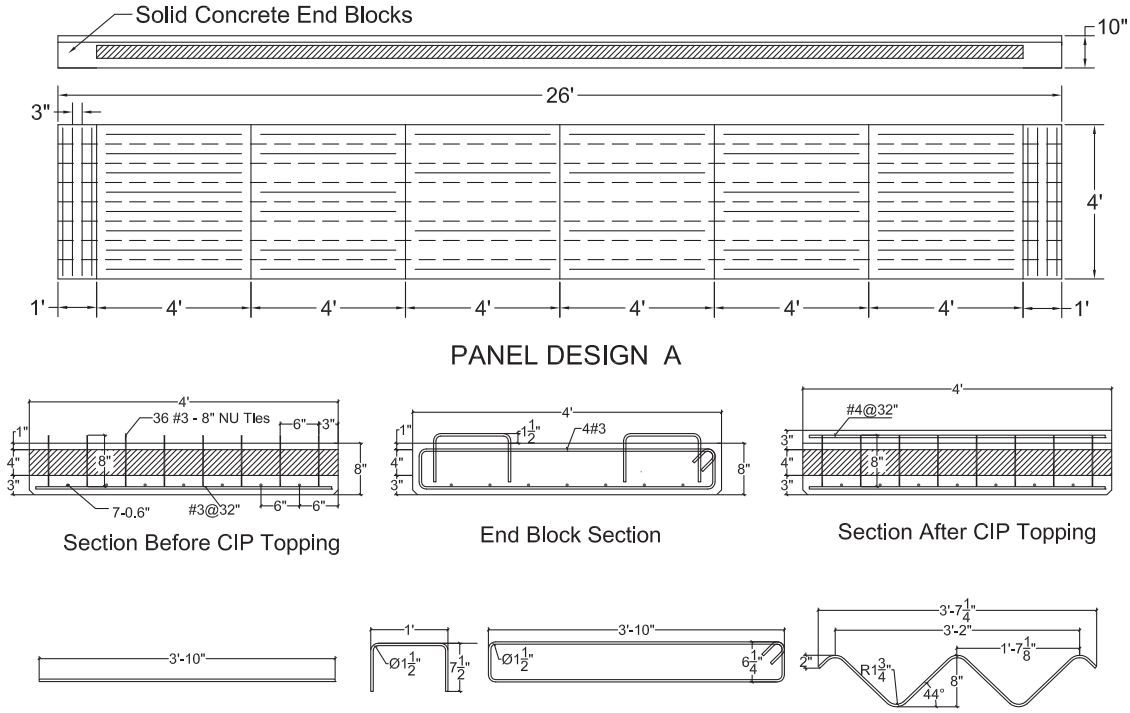

Fig. 1. Views and reinforcement of Panel Design A (1 ft = 0.305 m; 1 in. = 25.4 mm)

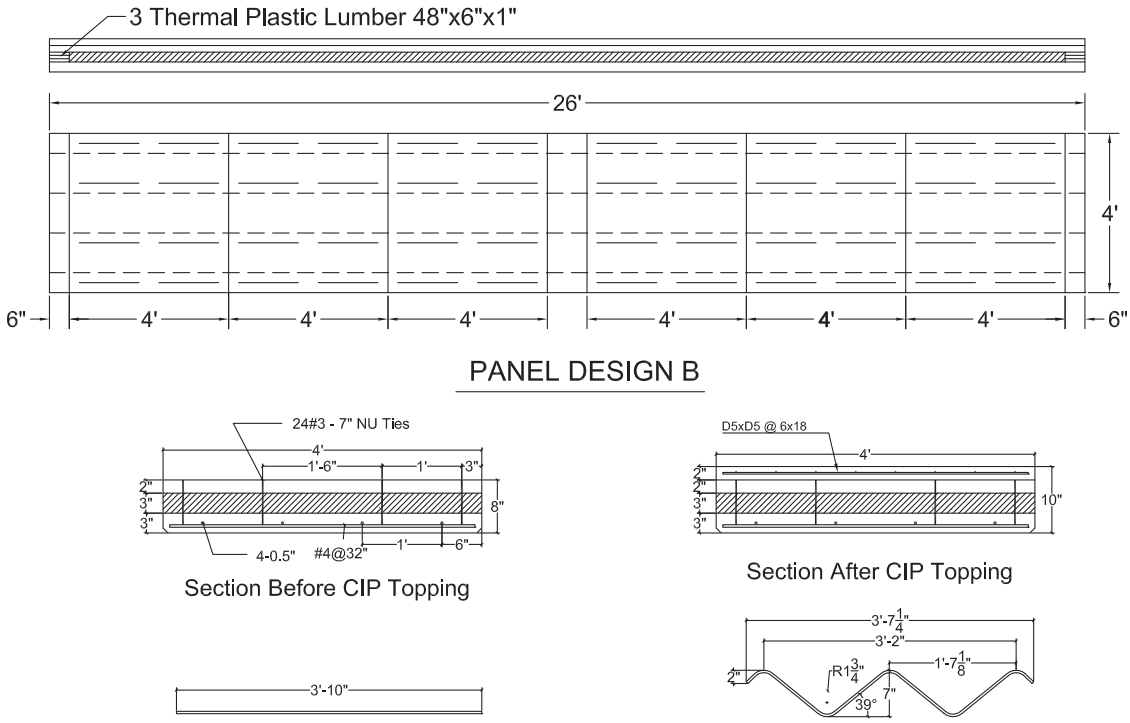

Fig. 2. Views and reinforcement of Panel Design B (1 ft = 0.305 m; 1 in. = 25.4 mm)

Thermal Analysis of the Proposed PCSP for Floors

GFRP ties typically have a thermal conductivity, $k = 0.062$ kcal/h/m/°C (0.5 Btu-in./h/sq ft/°F), which is much lower than that of concrete, $k = 1.65$ kcal/h/m/°C (13.3 Btu-in./h/sq ft/°F) and metal, $k = 38.9$ kcal/h/m/°C (314 Btu-in./h/sq ft/°F). To study the thermal performances of these panels, R-values are calculated using the zone method proposed by the *PCI design handbook*, 7th Edition, Section 11.1.6 [Prestressed Concrete Institute (PCI) 2010]. The *PCI design handbook* (PCI 2010) calculations resulted in a lower R-value for Panel Design A ($R = 10.2$) than for Panel Design B ($R = 11.4$), despite the use of

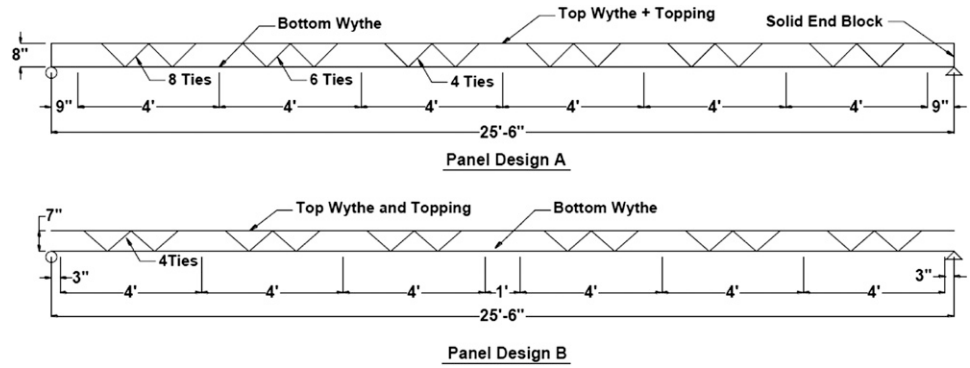

Fig. 3. Truss models of Panel Designs A and B (1 ft = 0.305 m; 1 in. = 25.4 mm)

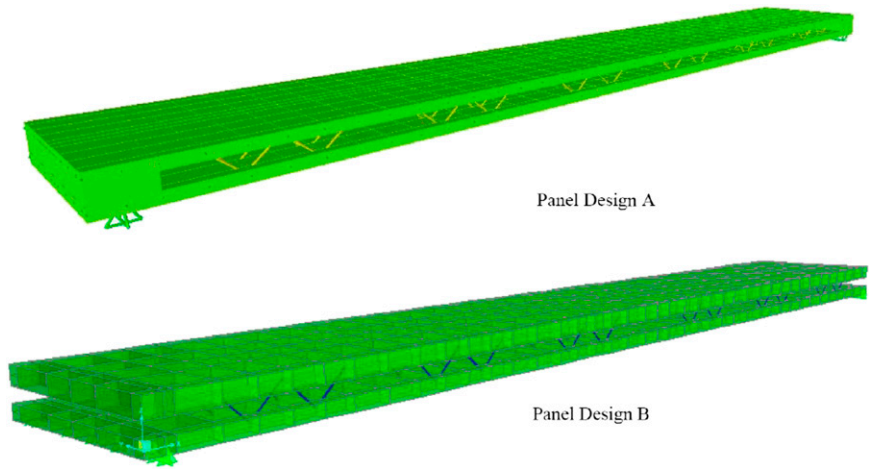

Fig. 4. Three-dimensional FE models of Panel Designs A and B

Table 1. Comparing Deflections Predicted Using Beam and Truss/FE Models

Panel design	Deflection calculation method	Precast only			Precast + 2-in. CIP topping
		Prestressing (mm)	Self-weight (mm)	Topping weight (mm)	Service loads (mm)
A	Beam model	−15.5	7.9	3.3	11.7
	Truss/FE model	−15.5	12.7	5.6	25.9
B	Beam model	−9.7	7.4	2.5	5.6
	Truss/FE model	−8.1	21.8	8.1	20.1

Note: Negative sign indicates camber (25.4 mm = 1 in.).

10-mm-thick (4-in.-thick) XPS in Panel Design A versus 75-mm-thick (3-in.-thick) XPS in Panel Design B. This highlights the negative impact of the solid concrete end blocks on the thermal efficiency of the panels. For more information, see Henin (2012).

Production of Panel Specimens

Three specimens (A1, B1, and B2) were fabricated in the structural laboratory of the UNL at the Peter Kiewit Institute (PKI) in Omaha, Nebraska. Specimen A1 is fabricated according to Panel Design A, and Specimens B1 and B2 are identical and fabricated according to Panel Design B. The general steps that should be followed in fabricating the proposed floor panel are as follows:

1. Prepare XPS panels by thermally cutting slots in each panel using hot blades as shown in Fig. 5. The number of slots and their location are according to the distribution of NU ties in each design.
2. Insert NU ties into the slots and fill the remaining gaps with canned expandable foam as shown in Fig. 6 to prevent concrete from creating thermal bridges through the gaps. Remove excess foam after it is fully expanded using a fine-tooth blade.
3. Erect the side and end forms in the prestressing bed, oil the forms, and install prestressing strands and bottom wythe reinforcement as shown in Fig. 7. In the case of Panel Design A, solid concrete ends are formed and transverse stirrups are installed.

Fig. 5. Slotting XPS panels for installing NU ties

Fig. 6. Inserting the NU ties and filling the slot gaps with expandable foam

4. Cast the bottom wythe of concrete using flowable high-slump or self-consolidating concrete, place the XPS panels with NU ties on the fresh concrete of the bottom wythe as shown in Fig. 8, place the top wythe reinforcement and concrete, and roughen the surface. If needed, lifting inserts are added to the top wythe and anchored to NU ties at the panel ends.
5. Cure the panel and release prestressing strands after reaching the required release strength. Then, erect the panels and place the topping concrete. Welded wire reinforcement (WWR) can be used to reinforce the composite topping, as shown in Fig. 9, if needed. For building floors, panels are erected adjacent to each other and the keyways are grouted similar to HC floor construction.

Fig. 7. Forming the panel and installing bottom wythe strands and reinforcement

Experimental Investigation

In this investigation, each of the three specimens (A1, B1, and B2) was tested as listed in Table 2. Specimen A1 was tested twice in flexure, that is, with and without composite topping; Specimen B1 was tested in both flexure and shear with composite topping; and Specimen B2 was tested only once in flexure with composite topping. The table also lists the age of the precast panel and CIP concrete topping at the time of testing and the corresponding concrete strengths. Fig. 10 shows the compressive strength versus age for the precast concrete and CIP concrete for all the three specimens. Panels B1 and B2 were fabricated simultaneously using the same concrete batch.

Testing of Specimen A1

Specimen A1 was tested in two stages: (1) precast panel without topping subjected to simulated construction loads and topping weight; and (2) precast panel with 50-mm (2-in.) composite CIP concrete topping subjected to simulated service loads. Fig. 11 shows the test setup and the panel instrumentation for the two flexural tests. Roller supports were placed 7.8 m (25.5 ft) center to center, and a concentrated load was applied at midspan of the panel using a spreader beam and hydraulic jack. A wire potentiometer was attached under the loading point to measure panel deflections, and concrete strain gauges were placed at the top and bottom surfaces to measure concrete strain. The top gauges were isolated from the spreader beam.

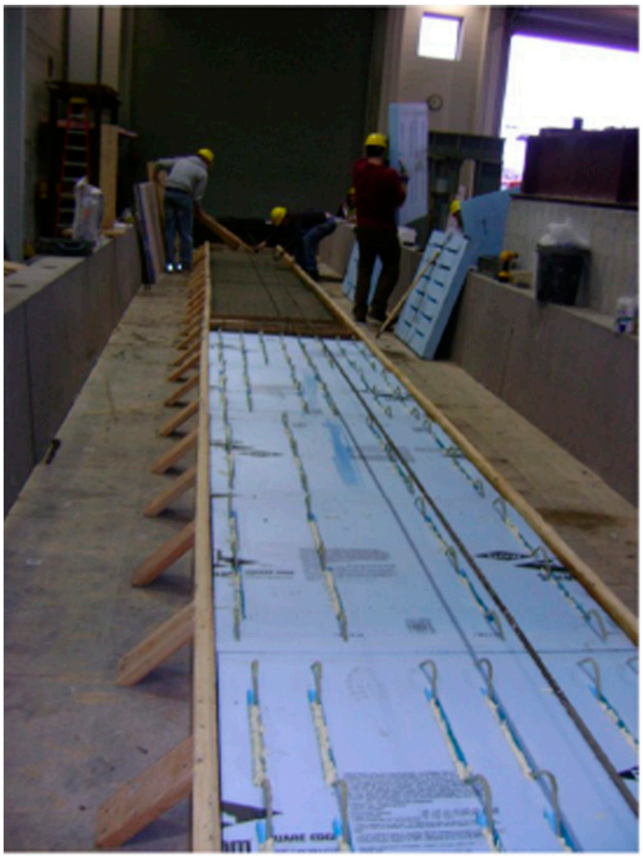

Fig. 8. Casting the bottom wythe and installing XPS panels

Fig. 9. Installing topping reinforcement on roughened surface before casting topping concrete

At the first stage, the panel is subjected to its self-weight [2.4 kPa (50 psf)] and a load that simulated the weight of CIP topping [1.2 kPa (25 psf)] and construction loads {[2.4 kPa (50 psf) according to ACI 347-04 [American Concrete Institute (ACI) 2004]}. Fig. 12 shows the load-deflection relationship for loading the precast panel up to the cracking load and unloading it. Fig. 12 also shows on the right vertical axis the equivalent uniform load, the load that results in the same deflections (in pounds per square foot). The net camber (after subtracting the self-weight deflection) was measured before testing and was approximately 6 mm (0.25 in.) upward, which is close to the value predicted using the truss/FE model in Table 1 after considering the *PCI design handbook* (PCI 2010) deflection multipliers [4 mm (0.17 in.)].

In the second stage of loading, Specimen A1 had a 50-mm (2-in.) composite CIP concrete topping. This test is to simulated additional superimposed dead and live loads, which are equal to 9.6 kPa (200 psf) for this panel design. Fig. 13 shows the load-deflection relationship, where the left vertical axis shows the applied load in pounds, whereas the right axis shows the corresponding uniform load, that is, the load that results in similar deflection, in pounds per square foot. The load-deflection relationship shows a linear behavior up to the cracking load, which was approximately 66.7 kN (15 kips). Nonlinear behavior then begins up to the ultimate load, which was approximately 148.52 kN (33.4 kips). The measured deflection under 9.6 kPa (200 psf) was 22 mm (0.85 in.), which is close to the value, predicted using the truss/FE model [26 mm (1.02 in.)] presented in Table 1. Also, the measured deflection under the 9.6 kPa (200 psf) load is within the L/360 deflection limit.

Prestress loss calculations were performed according to the 7th Edition of the *PCI design handbook* (PCI 2010), which resulted in a total prestress loss of approximately 18%. The nominal flexural capacity of the panel section (ϕM_n) was calculated using strain compatibility and assuming a fully composite section and resistance factor (ϕ) of 1.0. This resulted in a theoretical capacity of 306.4 kN·m (226 kip-ft), depth of compression block of 56 mm (2.22 in.), and ultimate stress in prestressing strands of 1,860 MPa (270 ksi). Under ultimate load [148.52 kN (33.4 kips)], the measured flexure moment at midspan section was 321.7 kN·m (237.3 kip-ft) (including self-weight moment), which indicates that the panel with solid end regions behaved as a fully composite section. In fact, its measured flexural capacity exceeded its calculated theoretical flexural capacity by 5%. Also, the ultimate strain in the concrete top fibers was measured to be 0.0022, which explains the tension-controlled flexural failure that occurred as shown in Fig. 14. Several cracks were observed on the top surface of the panel at each ends, which is mainly due to the restraint caused by the solid end blocks of the panel.

Testing of Specimen B1

Specimen B1 was tested in flexure after casting the 50-mm-thick (2-in.-thick) composite CIP concrete topping. This specimen and Specimen B2 had the composite topping applied shortly after casting the two wythes, that is, within about 4 days, to speed up the specimen fabrication. This specimen was designed, as shown in Fig. 2, to carry superimpose dead and live loads of 4.8 kPa (100 psf) and to be fully insulated, that is, no solid concrete end blocks. Flexural testing was performed by four-point loading as shown in Fig. 15. Concrete strain gauges were attached to the top surface at midspan to measure the

Table 2. Summary of the Test Program

Specimen ID	Test type	Description	Age of precast (days)	Age of topping (days)	$f'c$ precast (MPa)	$f'c$ topping (MPa)
A1	Flexure	Three-point loading of the precast panel (no composite topping)	5	N/A	64.8	N/A
	Flexure	Three-point loading of the composite panel	14	7	73.8	23.4
B1	Flexure	Four-point loading of the composite panel	19	15	79.3	41.4
	Shear	Three-point loading of 9-ft-long segment of the composite panel	23	19	82.0	41.4
B2	Flexure	Three-point loading of the composite panel	23	19	82.0	41.4

Note: 6.895 MPa = 1,000 psi.

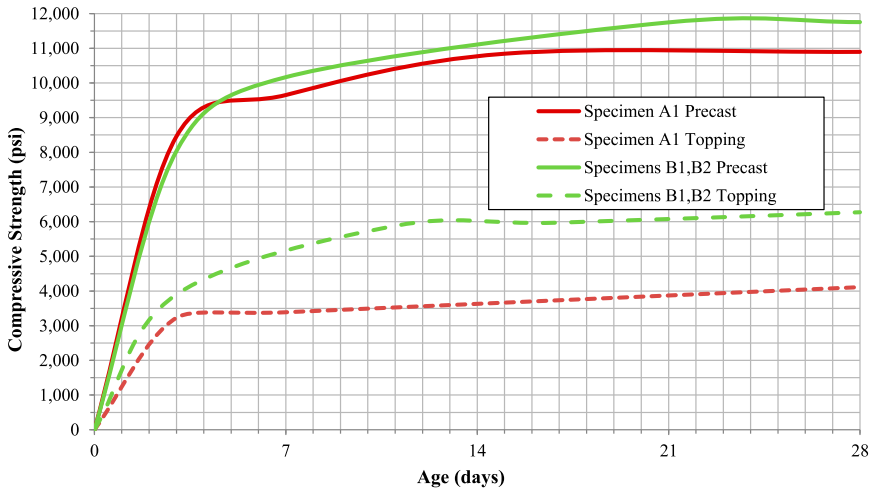

Fig. 10. Concrete strength development for the test specimens (1,000 lbs = 4.45 kN)

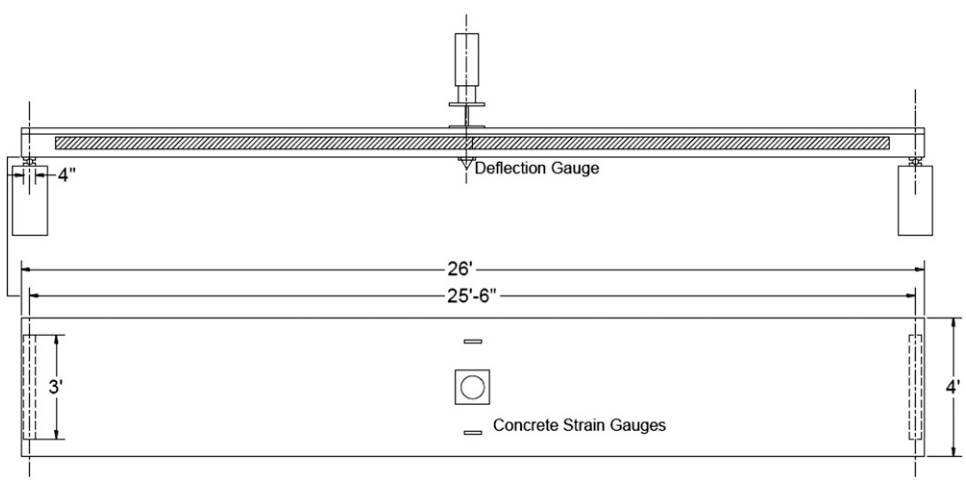

Fig. 11. Setup and instrumentation for the flexure testing of Precast Specimen A1 (1 ft = 0.305 m; 1 in. = 25.4 mm)

strain in extreme compression fibers and one potentiometer was located at midspan to measure deflection. To measure the strains in the NU ties, strain gauges were attached to the tension legs at the locations shown in Fig. 15. Also, an extensometer was attached to the panel at both ends to measure the relative movement between the top wythe and the bottom wythe.

Fig. 16 plots the load-deflection relationship of Specimen B1 tested in flexure. In this plot, the left vertical axis shows the applied load in pounds, whereas the right axis shows the corresponding uniform load that results in similar deflection (psf). This plot indicates that the specimen was able to carry 59.1 kN (13.3 kips) (total of two concentrated loads), which corresponds to a total measured flexure capacity equals to 120.4 kN·m (88.8 kip-ft), including the moment caused by the self-weight and topping weight. The required flexure capacity to resist the demand from factored loads is 116.9 kN (86.2 kip-ft), which is slightly below the

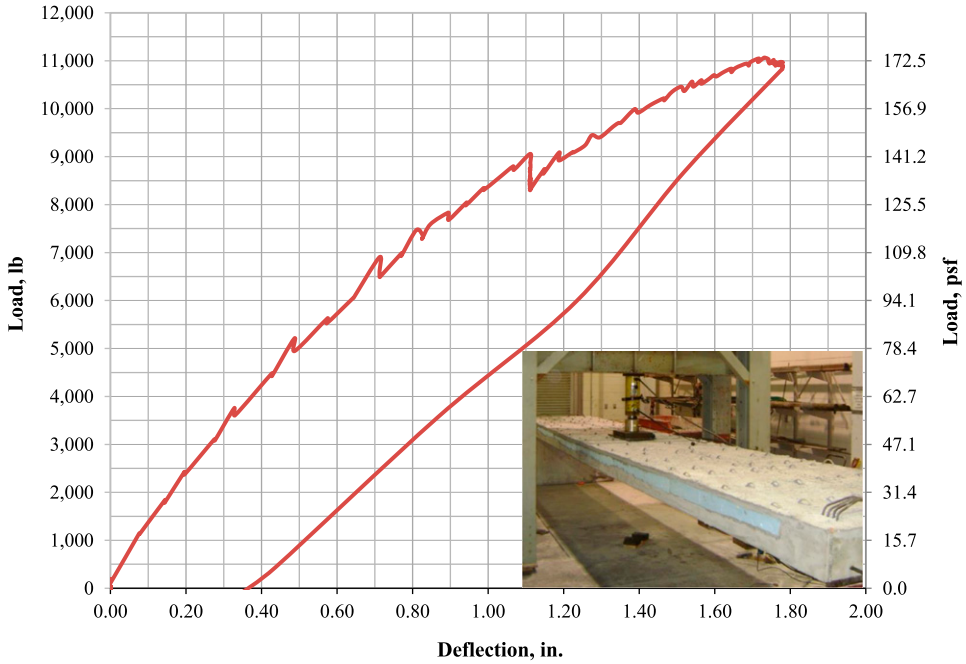

Fig. 12. Load-deflection relationships for Specimen A1 without topping (1,000 lbs = 4.45 kN; 1,000 psf = 0.04788 MPa)

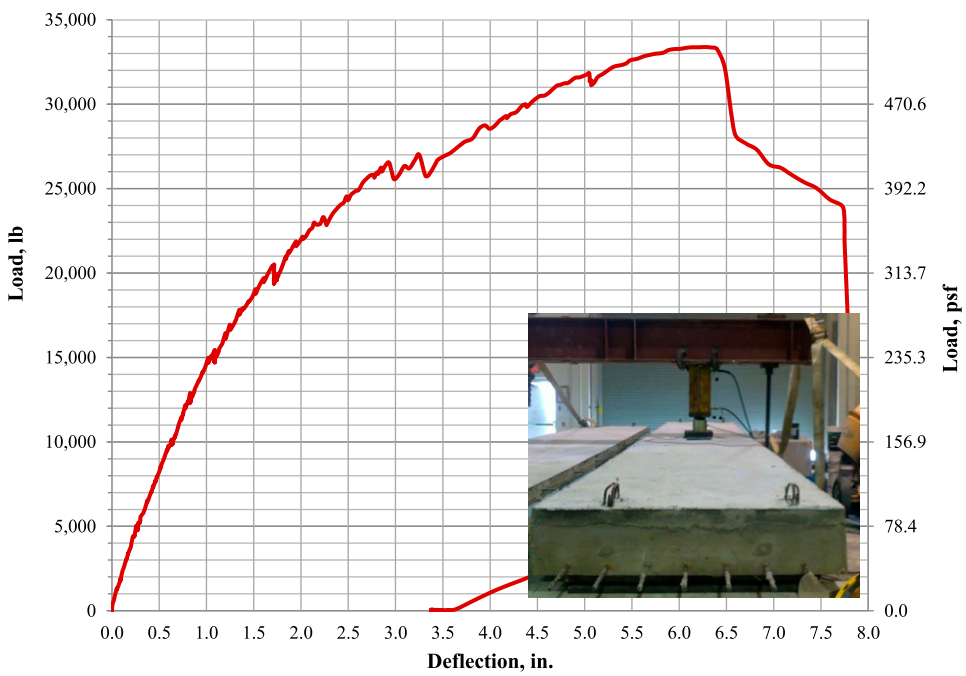

Fig. 13. Load-deflection relationship for Specimen A1 with composite topping (1,000 lbs = 4.45 kN; 1,000 psf = 0.04788 MPa)

measured flexure capacity. However, the nominal flexure capacity (theoretical flexure capacity with $\phi = 1$) of the specimen predicted using strain compatibility approach was found to be 152.4 kN·m (112.4 kip-ft), which is 26% higher than the measured flexure capacity. This significant drop in the specimen flexure capacity was primarily caused by the premature horizontal shear failure between the top and bottom wythes caused by pullout of ties from the bottom wythe. The failure condition is shown in Fig. 17. To determine the reason of the premature failure, the strains in all the ties were plotted as shown in Fig. 18. Fig. 18 indicates that the maximum strain in the tension legs of all ties was approximately 0.0067, which occurred at the ties located 0.91 and 2.1 m (3 and 7 ft) from the end of the specimen. This strain corresponds to a stress of approximately 277.2 MPa (40.2 ksi) using modulus of elasticity of 41.4 GPa (6,000 ksi). Fig. 18 also indicates that ties located 3.3 m (11 ft) from the end of the specimen had very low strains (less than 0.0008), which

correspond to a stress of approximately 33.1 MPa (4.8 ksi). This low stress is because the applied load produced no shear at the center part and the four ties located either side of the middle of the specimen between the loading points did not contribute to the horizontal shear resistance. Therefore, in the testing of Specimen B2, it was decided that this specimen should be tested using only one loading point at the midspan to engage the middle ties in resisting the horizontal shear forces and possibly achieve the flexure capacity of a fully composite panel.

Fig. 16 also indicates that the deflection of the specimen under service loads [4.8 kPa (100 psf)] is approximately 20 mm (0.8 in.), which is very close to the value predicted using the truss/FE model shown in Table 1. The maximum measured compressive strain in the concrete top fibers at midspan was 0.00046, which is significantly below the ultimate compressive strain of concrete (0.003). Fig. 19 shows the relative movement between the top and bottom wythes during testing. This relative moment indicates that the failure mode was the horizontal shear failure at one end of the specimen.

Fig. 14. Specimen A1 deformed shape under ultimate load

After flexure testing of Specimen B1, the middle 2.7 m (9 ft) of the specimen was removed to be tested in shear, because it did not experience any cracking or separation. Fig. 20 shows the test setup, where the load was applied at the middle of the 2.13-m span (7-ft span). Specimen deflection was recorded using one potentiometer located at the midspan; also, the strains in the GFRP ties were measured using strain gauges.

Fig. 21 plots the load-deflection relationships of the shear test for Specimen B1. This plot indicates that the specimen was able to carry 136.51 kN (30.7 kips), which corresponds to measured shear capacity of 73.8 kN (16.6 kips) (including the self-weight and topping weight). The demand shear capacity is 60 kN (13.5 kips), which is 27.7% less than the measured shear capacity.

The measured strain in the tension legs of NU ties indicates that the maximum strain is approximately 0.0108, which occurred in the ties located at the left side of the panel end as shown in Fig. 19. This strain corresponds to a stress of approximately 446.8 MPa (64.8 ksi) using a modulus of elasticity of 41.4 GPa (6,000 ksi). Fig. 22 shows the failure that occurred because of the horizontal shear, which resulted in the pullout of some ties from the bottom concrete wythe.

Testing Panel B2

Fig. 23 shows the test setup and instrumentation of Specimen B2. This specimen has exactly the same design of Specimen B1, but it was loaded with one concentrated load at the midspan to engage all the ties in the horizontal shear resistance as had been observed from testing Specimens A1 and B1. Strain gauges were attached to the top concrete surface at midspan and on the tension legs of NU ties as shown in Fig. 24. One potentiometer was located at the midspan to measure deflection and an extensometer was attached to the panel end to measure the relative movement between the top wythe and the bottom wythe.

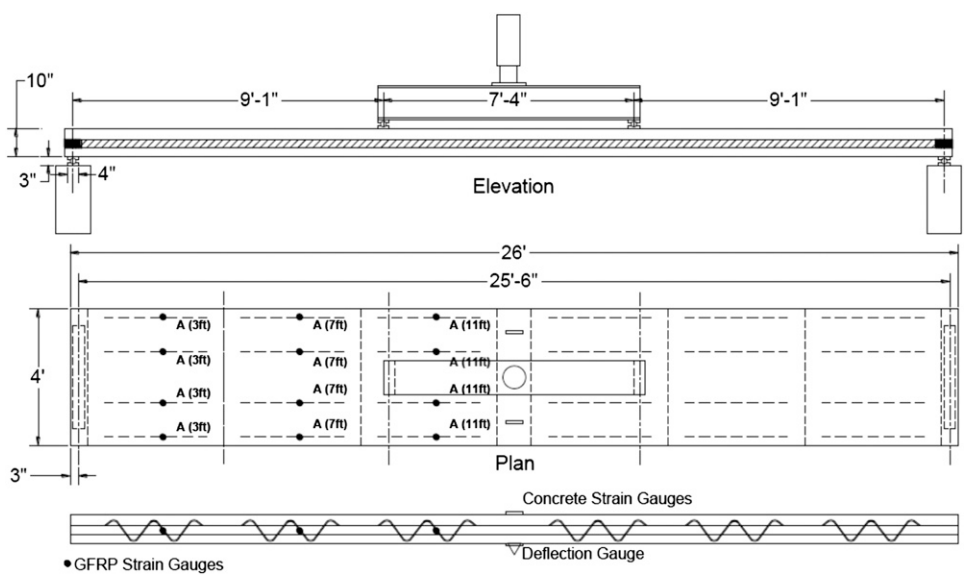

Fig. 15. Test setup and instrumentation of Specimen B1 (1 ft = 0.305 m; 1 in. = 25.4 mm)

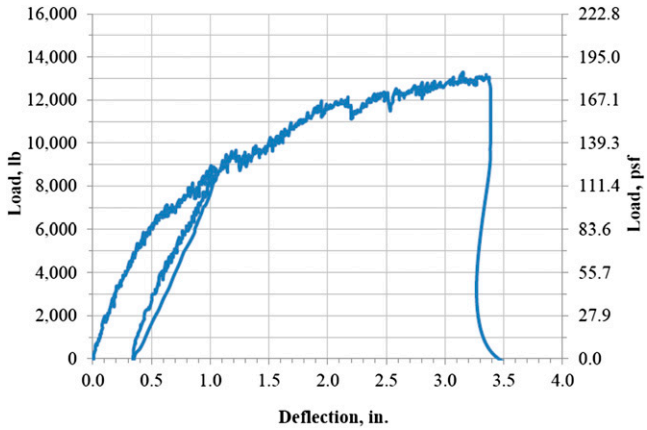

Fig. 16. Load-deflection relationship for flexure testing of Specimen B1 (1,000 lbs = 4.45 kN; 1,000 psf = 0.04788 MPa)

Fig. 17. Horizontal shear failure of Specimen B1 in flexure testing

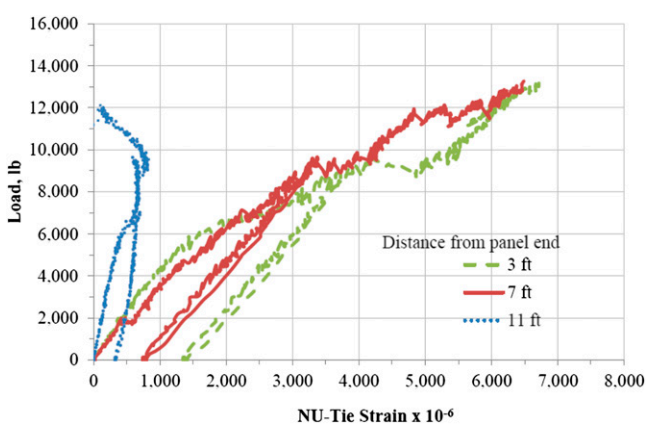

Fig. 18. Load-strain relationship for different ties in Specimen B1 (1,000 lbs = 4.45 kN; 1 ft = 0.305 m)

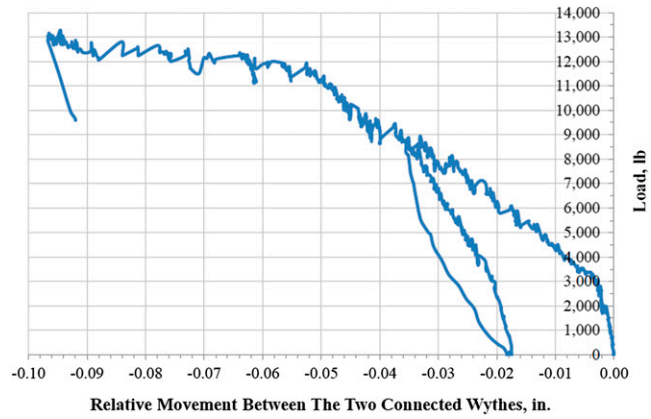

Fig. 19. Load-relative movement relationship for the wythes of Specimen B1 in flexure testing (1,000 lbs = 4.45 kN; 1 in. = 25.4 mm)

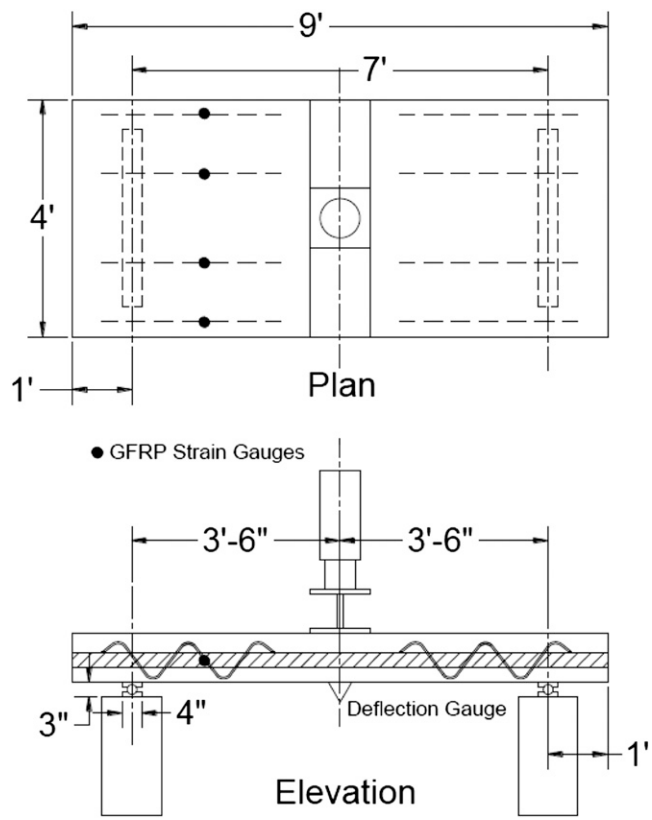

Fig. 20. Test setup and instrumentation of Specimen B1 for shear testing (1 ft = 0.305 m; 1 in. = 25.4 mm)

In this test, Specimen B2 was able to carry 66.7 kN (15 kips), which corresponds to a total measured flexure capacity of 168.25 kN·m (124.1 kip-ft) (including the moment caused by the self-weight and topping weight). The required flexure capacity for resisting the demand from factored loads ($1.2D + 1.6L$) is 116.9 kN·m (86.2 kip-ft), which is 30.5% less than the measured flexure capacity. Also, the nominal flexure capacity (theoretical flexure capacity with $\phi = 1$) of the specimen predicted using strain compatibility approach and assuming a fully composite section was found to be 152.1 kN·m (112.4 kip-ft), which is 9.4% less than the measure flexure capacity. Failure was by a tension-controlled

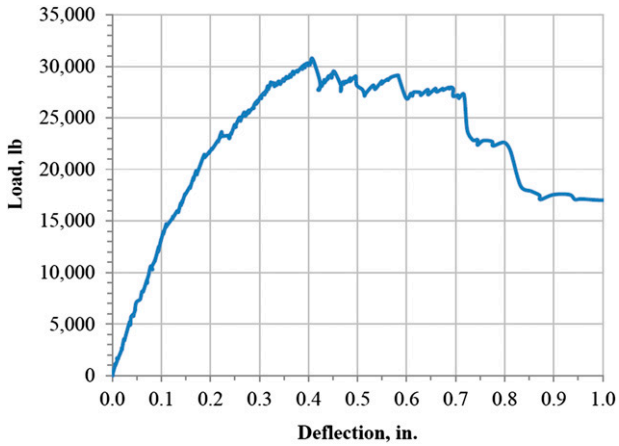

Fig. 21. Load-deflection relationship for the shear test of Specimen B1 (1,000 lbs = 4.45 kN; 1 in. = 25.4 mm)

Fig. 22. Shear failure of Specimen B1

ductile flexure failure, as shown in Fig. 24. Fig. 25 plots the strains in the tension legs of NU ties located at different distances from the panel ends. This figure indicates that the maximum strain in the tension legs of all ties ranged from 0.006 and 0.0074. This strain corresponds to a stress range from 248.2 to 306.1 MPa (36 to 44.4 ksi) using a modulus of elasticity of 6,000 ksi. This stress level indicates that all the ties in the span were being used in horizontal shear resistance, which resulted in a full-composite action between the top and bottom wythes. The maximum compressive strain in the concrete top fibers at midspan was 0.0016, which is below the ultimate compressive strain of 0.003 in the concrete. Fig. 26 shows the relative movement between the top and bottom wythes under ultimate load. This relative moment is indicative of a horizontal shear failure mode, which occurred at one end of the specimen. This test demonstrated the excellent structural performance of the proposed floor panels.

Table 3 lists the theoretical and measured flexural capacity of the three tested specimens, as well as the ratio of measured to theoretical capacities. The theoretical capacities were calculated using strain compatibility and assuming a fully composite section with a resistance factor of 1.0. The presented ratios indicate that the ultimate strength of Specimens A1 and B2 (testing using three-point loading) exceeded the theoretical capacity. The flexure capacity of Specimen B1 (tested using four-point loading) was lower than predicted because the shear connectors located between the two applied loads did not contribute to horizontal shear resistance, which resulted in premature horizontal shear failure.

Conclusions and Recommendations

On the basis of the results of the experimental and analytical investigations, the following conclusions are made:

1. The fabrication of proposed floor panels using the procedure presented in the paper is simple, efficient, economical, and does not require specialized equipment.
2. The number of ties required to achieve full composite action should be calculated using the *PCI design handbook* (PCI 2010) method for horizontal shear in composite members. The

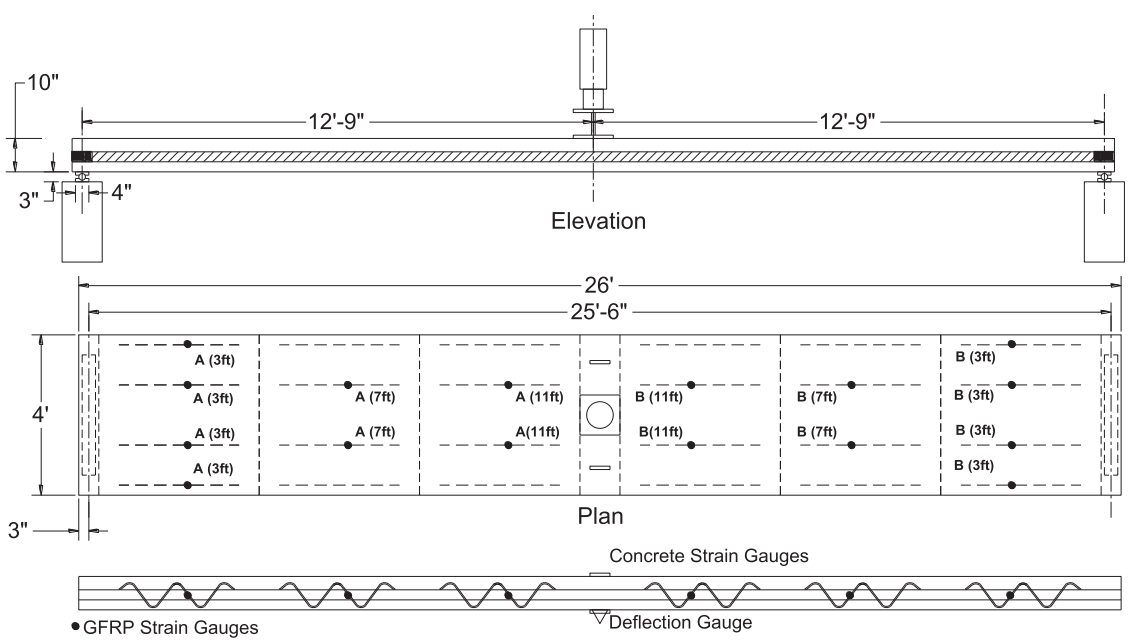

Fig. 23. Test setup and instrumentation of Panel B2 (1 ft = 0.305 m; 1 in. = 25.4 mm)

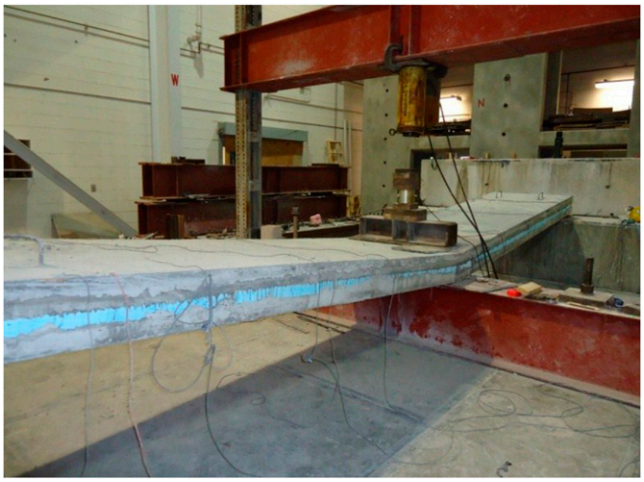

Fig. 24. Flexure failure of Specimen B2

most efficient distribution of ties is the one that corresponds to the shear force diagram. For example, it is more efficient to use more ties at the panel ends than toward the middle of the panel in case of uniform load.

3. The proposed floor panels can behave as fully composite members under ultimate load provided the shear ties are appropriately distributed. It is not necessary to have solid blocks of concrete connecting the wythes. The theoretical ultimate flexural capacity can be calculated using strain compatibility.
4. Calculating deflections of the proposed floor panels using the truss/FE models results in more realistic deflection predictions than using a beam flexural model.

For designing the proposed floor system, it is recommended to first estimate the number of shear connectors (ties) required to achieve the full-composite action between the top and bottom wythes. Then, a two-dimensional (2D) truss model should be developed and analyzed to determine deflection behavior under superimposed loads. Otherwise, a conservative stiffness reduction factor may be used with

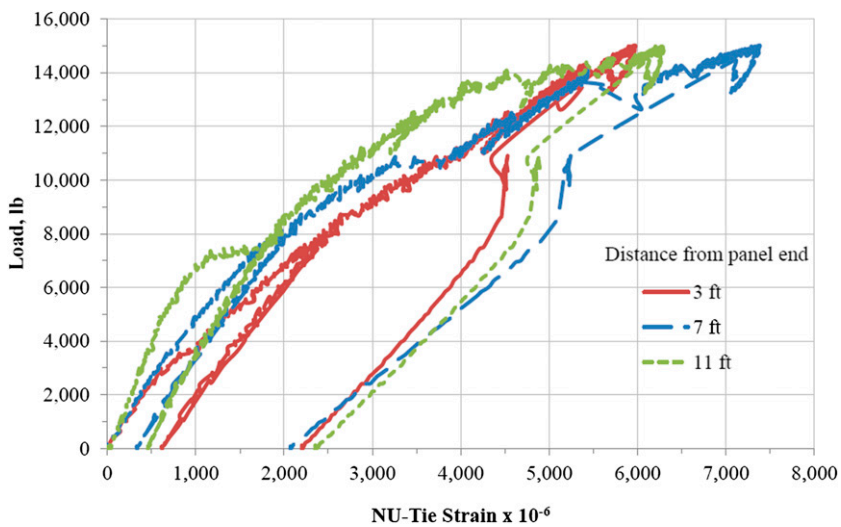

Fig. 25. Load-strain relationship of NU ties in flexure testing of Specimen B2 (1,000 lbs = 4.45 kN; 1 ft = 0.305 m)

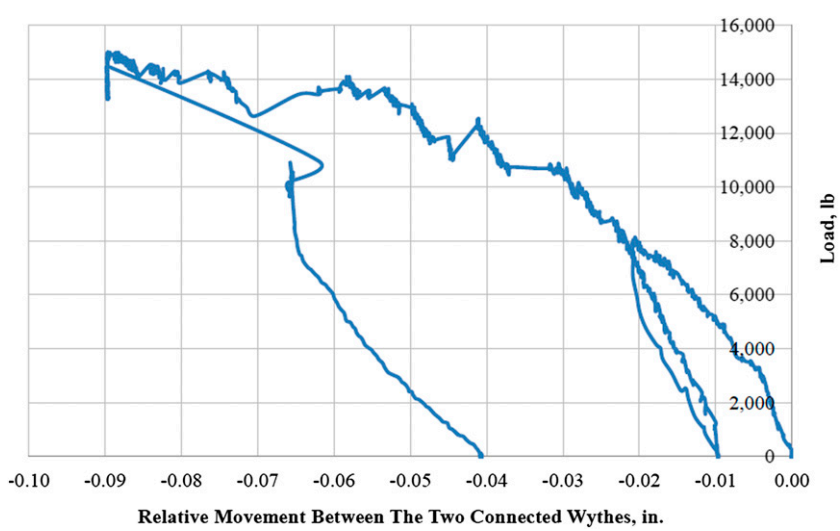

Fig. 26. Load-relative movement relationship for the wythes of Specimen B2 in flexure testing (1,000 lbs = 4.45 kN; 1 in. = 25.4 mm)

Table 3. Summary of Flexure Testing Results for the Three Specimens

Specimen	L_e (m)	$M_{\text{theoretical}}$ (kN·m)	$W_{S.W}$ (kN/m)	$M_{S.W}$ (kN·m)	P_{measured} (kN)	M_{measured} (kN·m)	$M_{\text{total.measured}}$ (kN·m)	$M_{\text{total.measured}}/M_{\text{theoretical}}$
A1	7.823	306.5	4.550	34.8	148.6	290.7	325.5	1.06
B1	7.722	151.9	5.104	38.0	59.2	81.2	119.2	0.79
B2	7.722	151.9	5.104	38.0	66.8	128.9	166.9	1.10

Note: 25.4 mm = 1 in.; 4.45 kN = 1 kip; 0.113 kN·m = 1 kip-in.; 175 kN/m = 1 kip/in. L_e = effective span of panel; $M_{S.W}$ = bending moment due to panel self-weight; $W_{S.W}$ = uniform load representing panel self-weight.

the beam model. Stresses in shear connectors caused by sustained load should be checked against the creep limits.

References

Al-Einea, A., Salmon, D. C., Tadros, M. K., Culp, T., and Fogarasi, G. J. (1991). "State-of-the-art of precast concrete sandwich panels." *PCI J.*, 36(6), 78–98.

American Concrete Institute (ACI). (2004). "Guide to formwork for concrete." *ACI 347-04,* Farmington Hills, MI.

Federation International Du Beton Steering Committee. (2000). "Special design consideration for precast prestressed hollow core floors." *Technical Bulletin No. 6*, FIB, Lausanne, Switzerland.

Hanlon, J., Dolan, C. W., Figurdki, D., Deng, J., and Dolan, J. G. (2009). "Precast concrete building system components for the Westin Resort Hotel: Part 1." *PCI J.*, 54(2), 88–96.

Hanna, K., Henin, E., Toneies, N., Morcous, G., and Tadros, M. K. (2011). "Design, detailing, and testing of cladding panels using GFRP ties." *Proc., PCI 57th Annual Convention*, Precast/Prestressed Concrete Institute, Chicago.

Henin, E. (2012). "Efficient precast/prestressed concrete floor system for building construction." Ph.D. dissertation, Univ. of Nebraska–Lincoln, Omaha, NE.

Henin, E., Morcous, G., and Tadros, M. K. (2011). "Precast concrete sandwich panels for floor and roof applications." *Proc., PCI 57th Annual Convention*, Precast/Prestressed Concrete Institute, Chicago.

Mid-State Filigree Systems. (1992). *The filigree wideslab method of concrete deck construction*, Cranbury, NJ.

Morcous, G., Henin, E., Lafferty, M., and Tadros, M. K. (2011). "Design and testing of tornado-resistant precast/prestressed concrete sandwich panels with GFRP ties." *Proc., PCI 57th Annual Convention*, Precast/Prestressed Concrete Institute, Chicago.

Morcous, G., Tadros, M. K., Lafferty, M., and Gremel, D. (2010). "Optimized sandwich panel system for energy, composite action and production efficiency." *Proc., 3rd fib Int. Congress*, Precast/Prestressed Concrete Institute, Chicago.

Prestressed Concrete Institute (PCI). (2010). *PCI design handbook*, 7th Ed., Chicago.

Song, X., Morcous, G., Lafferty, M., Gremel, D., and Tadros, M. K. (2009). "Effect of NU-tie distribution on the composite action of precast/prestressed concrete sandwich panels." *Proc., PCI Annual Convention*, Precast/Prestressed Concrete Institute, Chicago.